

NANOCIÊNCIAS E NANOTECNOLOGIA:

Pesquisa e Aplicações

Juan Ramón Collet-Lacoste
(Organizador)



**EDITORIA
ARTEMIS**

2022

NANOCIÊNCIAS E NANOTECNOLOGIA:

Pesquisa e Aplicações

Juan Ramón Collet-Lacoste
(Organizador)



**EDITORIA
ARTEMIS**

2022



O conteúdo deste livro está licenciado sob uma Licença de Atribuição Creative Commons Atribuição-Não-Comercial NãoDerivativos 4.0 Internacional (CC BY-NC-ND 4.0). Direitos para esta edição cedidos à Editora Artemis pelos autores. Permitido o download da obra e o compartilhamento, desde que sejam atribuídos créditos aos autores, e sem a possibilidade de alterá-la de nenhuma forma ou utilizá-la para fins comerciais.

A responsabilidade pelo conteúdo dos artigos e seus dados, em sua forma, correção e confiabilidade é exclusiva dos autores. A Editora Artemis, em seu compromisso de manter e aperfeiçoar a qualidade e confiabilidade dos trabalhos que publica, conduz a avaliação cega pelos pares de todos manuscritos publicados, com base em critérios de neutralidade e imparcialidade acadêmica.

Editora Chefe	Prof. ^a Dr. ^a Antonella Carvalho de Oliveira
Editora Executiva	M. ^a Viviane Carvalho Mocellin
Direção de Arte	M. ^a Bruna Bejarano
Diagramação	Elisangela Abreu
Organizador	Prof. Dr. Juan Ramón Collet-Lacoste
Imagem da Capa	Liuzishan/123RF
Bibliotecária	Janaina Ramos – CRB-8/9166

Conselho Editorial

Prof.^a Dr.^a Ada Esther Portero Ricol, *Universidad Tecnológica de La Habana “José Antonio Echeverría”*, Cuba
Prof. Dr. Adalberto de Paula Paranhos, Universidade Federal de Uberlândia
Prof.^a Dr.^a Amanda Ramalho de Freitas Brito, Universidade Federal da Paraíba
Prof.^a Dr.^a Ana Clara Monteverde, *Universidad de Buenos Aires, Argentina*
Prof.^a Dr.^a Ana Júlia Viamonte, Instituto Superior de Engenharia do Porto (ISEP), Portugal
Prof. Dr. Ángel Mujica Sánchez, *Universidad Nacional del Altiplano, Peru*
Prof.^a Dr.^a Angela Ester Mallmann Centenaro, Universidade do Estado de Mato Grosso
Prof.^a Dr.^a Begoña Blandón González, *Universidad de Sevilla, Espanha*
Prof.^a Dr.^a Carmen Pimentel, Universidade Federal Rural do Rio de Janeiro
Prof.^a Dr.^a Catarina Castro, Universidade Nova de Lisboa, Portugal
Prof.^a Dr.^a Cirila Cervera Delgado, *Universidad de Guanajuato, México*
Prof.^a Dr.^a Cláudia Padovesi Fonseca, Universidade de Brasília-DF
Prof.^a Dr.^a Cláudia Neves, Universidade Aberta de Portugal
Prof. Dr. Cleberton Correia Santos, Universidade Federal da Grande Dourados
Prof. Dr. David García-Martul, *Universidad Rey Juan Carlos de Madrid, Espanha*
Prof.^a Dr.^a Deuzimar Costa Serra, Universidade Estadual do Maranhão
Prof.^a Dr.^a Dina Maria Martins Ferreira, Universidade Estadual do Ceará
Prof.^a Dr.^a Eduarda Maria Rocha Teles de Castro Coelho, Universidade de Trás-os-Montes e Alto Douro, Portugal
Prof. Dr. Eduardo Eugênio Spers, Universidade de São Paulo
Prof. Dr. Eloi Martins Senhoras, Universidade Federal de Roraima, Brasil



Prof.ª Dr.ª Elvira Laura Hernández Carballido, *Universidad Autónoma del Estado de Hidalgo*, México
Prof.ª Dr.ª Emilas Darlene Carmen Lebus, *Universidad Nacional del Nordeste/ Universidad Tecnológica Nacional*, Argentina
Prof.ª Dr.ª Erla Mariela Morales Morgado, *Universidad de Salamanca*, Espanha
Prof. Dr. Ernesto Cristina, *Universidad de la República*, Uruguay
Prof. Dr. Ernesto Ramírez-Briones, *Universidad de Guadalajara*, México
Prof. Dr. Gabriel Díaz Cobos, *Universitat de Barcelona*, Espanha
Prof.ª Dr.ª Gabriela Gonçalves, Instituto Superior de Engenharia do Porto (ISEP), Portugal
Prof. Dr. Geoffroy Roger Pointer Malpass, Universidade Federal do Triângulo Mineiro, Brasil
Prof.ª Dr.ª Gladys Esther Leoz, *Universidad Nacional de San Luis*, Argentina
Prof.ª Dr.ª Glória Beatriz Álvarez, *Universidad de Buenos Aires*, Argentina
Prof. Dr. Gonçalo Poeta Fernandes, Instituto Politécnico da Guarda, Portugal
Prof. Dr. Gustavo Adolfo Juarez, *Universidad Nacional de Catamarca*, Argentina
Prof.ª Dr.ª Iara Lúcia Tescarollo Dias, Universidade São Francisco, Brasil
Prof.ª Dr.ª Isabel del Rosario Chiyon Carrasco, *Universidad de Piura*, Peru
Prof.ª Dr.ª Isabel Yohena, *Universidad de Buenos Aires*, Argentina
Prof. Dr. Ivan Amaro, Universidade do Estado do Rio de Janeiro, Brasil
Prof. Dr. Iván Ramon Sánchez Soto, *Universidad del Bío-Bío*, Chile
Prof.ª Dr.ª Ivânia Maria Carneiro Vieira, Universidade Federal do Amazonas, Brasil
Prof. Me. Javier Antonio Albornoz, *University of Miami and Miami Dade College*, Estados Unidos
Prof. Dr. Jesús Montero Martínez, *Universidad de Castilla - La Mancha*, Espanha
Prof. Dr. João Manuel Pereira Ramalho Serrano, Universidade de Évora, Portugal
Prof. Dr. Joaquim Júlio Almeida Júnior, UniFIMES - Centro Universitário de Mineiros, Brasil
Prof. Dr. José Cortez Godínez, Universidad Autónoma de Baja California, México
Prof. Dr. Juan Carlos Cancino Diaz, Instituto Politécnico Nacional, México
Prof. Dr. Juan Carlos Mosquera Feijoo, *Universidad Politécnica de Madrid*, Espanha
Prof. Dr. Juan Diego Parra Valencia, *Instituto Tecnológico Metropolitano de Medellín*, Colômbia
Prof. Dr. Juan Manuel Sánchez-Yáñez, *Universidad Michoacana de San Nicolás de Hidalgo*, México
Prof. Dr. Júlio César Ribeiro, Universidade Federal Rural do Rio de Janeiro, Brasil
Prof. Dr. Leinig Antonio Perazolli, Universidade Estadual Paulista (UNESP), Brasil
Prof.ª Dr.ª Livia do Carmo, Universidade Federal de Goiás, Brasil
Prof.ª Dr.ª Luciane Spanhol Bordignon, Universidade de Passo Fundo, Brasil
Prof. Dr. Luis Fernando González Beltrán, Universidad Nacional Autónoma de México, México
Prof. Dr. Luis Vicente Amador Muñoz, *Universidad Pablo de Olavide*, Espanha
Prof.ª Dr.ª Macarena Esteban Ibáñez, *Universidad Pablo de Olavide*, Espanha
Prof. Dr. Manuel Ramiro Rodríguez, *Universidad Santiago de Compostela*, Espanha
Prof.ª Dr.ª Márcia de Souza Luz Freitas, Universidade Federal de Itajubá, Brasil
Prof. Dr. Marcos Augusto de Lima Nobre, Universidade Estadual Paulista (UNESP), Brasil
Prof. Dr. Marcos Vinicius Meiado, Universidade Federal de Sergipe, Brasil
Prof.ª Dr.ª Mar Garrido Román, *Universidad de Granada*, Espanha
Prof.ª Dr.ª Margarida Márcia Fernandes Lima, Universidade Federal de Ouro Preto, Brasil
Prof.ª Dr.ª Maria Aparecida José de Oliveira, Universidade Federal da Bahia, Brasil
Prof.ª Dr.ª Maria Carmen Pastor, *Universitat Jaume I*, Espanha
Prof.ª Dr.ª Maria do Céu Caetano, Universidade Nova de Lisboa, Portugal
Prof.ª Dr.ª Maria do Socorro Saraiva Pinheiro, Universidade Federal do Maranhão, Brasil
Prof.ª Dr.ª Maria Lúcia Pato, Instituto Politécnico de Viseu, Portugal

Prof.^a Dr.^a Maritza González Moreno, *Universidad Tecnológica de La Habana*, Cuba
Prof.^a Dr.^a Mauriceia Silva de Paula Vieira, Universidade Federal de Lavras, Brasil
Prof.^a Dr.^a Odara Horta Boscolo, Universidade Federal Fluminense, Brasil
Prof. Dr. Osbaldo Turpo-Gebera, *Universidad Nacional de San Agustín de Arequipa*, Peru
Prof.^a Dr.^a Patrícia Vasconcelos Almeida, Universidade Federal de Lavras, Brasil
Prof.^a Dr.^a Paula Arcoverde Cavalcanti, Universidade do Estado da Bahia, Brasil
Prof. Dr. Rodrigo Marques de Almeida Guerra, Universidade Federal do Pará, Brasil
Prof. Dr. Saulo Cerqueira de Aguiar Soares, Universidade Federal do Piauí, Brasil
Prof. Dr. Sergio Bitencourt Araújo Barros, Universidade Federal do Piauí, Brasil
Prof. Dr. Sérgio Luiz do Amaral Moretti, Universidade Federal de Uberlândia, Brasil
Prof.^a Dr.^a Silvia Inés del Valle Navarro, *Universidad Nacional de Catamarca*, Argentina
Prof.^a Dr.^a Solange Kazumi Sakata, Instituto de Pesquisas Energéticas e Nucleares. Universidade de São Paulo (USP), Brasil
Prof.^a Dr.^a Teresa Cardoso, Universidade Aberta de Portugal
Prof.^a Dr.^a Teresa Monteiro Seixas, Universidade do Porto, Portugal
Prof. Dr. Valter Machado da Fonseca, Universidade Federal de Viçosa, Brasil
Prof.^a Dr.^a Vanessa Bordin Viera, Universidade Federal de Campina Grande, Brasil
Prof.^a Dr.^a Vera Lúcia Vasilévski dos Santos Araújo, Universidade Tecnológica Federal do Paraná, Brasil
Prof. Dr. Wilson Noé Garcés Aguilar, *Corporación Universitaria Autónoma del Cauca*, Colômbia

Dados Internacionais de Catalogação na Publicação (CIP)

N186 Nanociências e nanotecnologia: pesquisa e aplicações /
Organizador Juan Ramón Collet-Lacoste. – Curitiba-
PR: Artemis, 2022.

Formato: PDF

Requisitos de sistema: Adobe Acrobat Reader

Modo de acesso: World Wide Web

Inclui bibliografia

ISBN 978-65-87396-66-8

DOI 10.37572/EdArt_290822668

1. Nanociência. 2. Nanotecnologia. 3. Pesquisa. I.
Collet-Lacoste, Juan Ramón (Organizador). II. Título.

CDD 620.5

Elaborado por Bibliotecária Janaina Ramos – CRB-8/9166



PRÓLOGO

Las propiedades particulares de las Nps, muy diferentes en muchos aspectos a las de sus sólidos masivos, han abierto nuevos campos de estudio e investigación a todo nivel: teóricos y aplicados. Son más inestables que los sólidos masivos de los que se diferencian principalmente por su estructura electrónica que no suele ser continua. Esto es una ventaja a nivel de su reactividad y suelen presentar superficies específicas altas que son muy propicias para los procesos de catálisis, un ingrediente muy importante en los procesos cinéticos. Otra propiedad interesante es que no presentan defectos estructurales en su volumen como vacancias o dislocaciones, a diferencia de sus correspondientes sólidos masivos.

Las presentes monografías forman parte del título: “Nanociências e Nanotecnologia: Pesquisa e Aplicações”. Los artículos están ordenados de lo más general (e.g., producción y caracterización de las Nps) a los relacionados con aplicaciones prácticas (e.g., foto catálisis y a su relación principalmente con aplicaciones de origen biológico).

Estos muestran la potencialidad de las nanotecnologías en la comprensión de nuevas aplicaciones en campos tan variados como la catálisis, fotocátalisis, bio-remediación, contaminantes, ambientes acuáticos, antisépticos, bactericidas, virucidas, compuestos bio-activos, biosíntesis extracelular e intracelular, estudio de suelos, vegetales y probióticos, etc.

Juan Ramón Collet-Lacoste

SUMÁRIO

CAPÍTULO 1..... 1

THE FOLLOWING NEW CONSIDERATIONS ON THE FINKE CHEMICAL MECHANISM OF NANOPARTICLE SYNTHESIS FOR TRANSITION METALS

Juan Ramón Collet-Lacoste

Jorge Javier Acosta

Pablo César Favilla

 https://doi.org/10.37572/EdArt_2908226681

CAPÍTULO 2.....28

SÍNTESE E CARACTERIZAÇÃO MORFOLÓGICA DE NANOESTRUTURAS DE $Ce_{1-x}Pr_xO_2$

Ana Cristina Tolentino Cabral

Isabela Cristina Fernandes Vaz

Francisco Moura Filho

 https://doi.org/10.37572/EdArt_2908226682

CAPÍTULO 3..... 39

SÍNTESE E SEPARAÇÃO DE NANOPARTÍCULAS DE PRATA USANDO POLIVINILPIRROLIDONA EM DIMETILFORMAMIDA

Celly Mieko Shinohara Izumi

Beatriz Rocha de Moraes

 https://doi.org/10.37572/EdArt_2908226683

CAPÍTULO 4..... 49

REDUÇÃO DO ÓXIDO DE GRAFENO VIA RADIAÇÃO IONIZANTE

Solange Kazumi Sakata

Raynara Maria Silva Jacovone

 https://doi.org/10.37572/EdArt_2908226684

CAPÍTULO 5..... 61

APLICAÇÃO DE NANOPARTÍCULAS METÁLICAS E BIMETÁLICAS EM FOTOCATÁLISE

Luelc Souza da Costa

Rômulo Batista Vieira

Diego Rodrigues de Carvalho

Elayne Valério Carvalho

 https://doi.org/10.37572/EdArt_2908226685

CAPÍTULO 6.....87

COMPLEX OXIDATION OF TMB CATALYZED WITH PEROXIDASE-LIKE AU NANOPARTICLES

Zhiming Liu

Wenjian Wu

 https://doi.org/10.37572/EdArt_2908226686

CAPÍTULO 7..... 98

USE OF NANOPARTICLES IN THE DEGRADATION OF CONTAMINANTS IN AQUATIC ENVIRONMENTS

Janet Jan-Roblero

Juan A. Cruz-Maya

Axel A. Treviño-Trejo

Oliver Navarrete-Godínez

Hugo A. Álvarez-Hernández

 https://doi.org/10.37572/EdArt_2908226687

CAPÍTULO 8..... 108

SÍNTESIS DE NANOPARTÍCULAS DE SULFURO DE CADMIO MEDIANTE UN SISTEMA ACUOSO DE BIOMASA FÚNGICA

Norma Gabriela Rojas Avelizapa

María Oliva Hernández Jiménez

Luz Irene Rojas Avelizapa

Héctor Paul Reyes Pool

 https://doi.org/10.37572/EdArt_2908226688

CAPÍTULO 9..... 116

ESTUDIO DE LAS NANOPARTÍCULAS DE SULFURO DE CADMIO OBTENIDAS A PARTIR DE BIOMASA Y EXTRACTOS FÚNGICOS DE *Fusarium oxysporum*

Diana Alexandra Calvo Olvera

José Daniel Aguilar Loa

Norma Gabriela Rojas Avelizapa

 https://doi.org/10.37572/EdArt_2908226689

CAPÍTULO 10.....126

ELABORATION OF AN ANTISEPTIC GEL BASED ON BIOACTIVE COMPOUNDS OF *ORIGANUM VULGARE* AND *ALOE VERA* ENCAPSULATED IN SiO₂ Y ZnO-SnO₂ NANOPARTICLES FOR CONTROLLED RELEASE

Guadalupe Luna Cedillo

Francisco Javier Tzompantzi Morales

Sandra Luz Hernández Valladolid

Juan Manuel Padilla Flores

 https://doi.org/10.37572/EdArt_29082266810

CAPÍTULO 11.....135

Bacillus thuringiensis AND *Micromonospora echinospora* IN *Lactuca sativa* OPTIMIZE NITROGENOUS FERTILIZER WITH A CRUDE EXTRACT OF CARBON NANOPARTICLES

Juan Luis Ignacio-De la Cruz

Juan Manuel Sánchez-Yañez

 https://doi.org/10.37572/EdArt_29082266811

SOBRE EL ORGANIZADOR.....143

ÍNDICE REMISSIVO 144

CAPÍTULO 1

THE FOLLOWING NEW CONSIDERATIONS ON THE FINKE CHEMICAL MECHANISM OF NANOPARTICLE SYNTHESIS FOR TRANSITION METALS

Data de submissão: 07/09/2021

Data de aceite: 24/09/2021

Juan Ramón Collet-Lacoste¹

Comisión Nacional de Energía Atómica
U.A.M. Div. Corrosión
Av. Gral. Paz 1499
Prov. de Buenos Aires
San Martín B1650KNA
Argentina
<https://orcid.org/0000-0003-3720-2231>

Jorge Javier Acosta

YPF Tecnología S.A
EE.RR. Av. Del Petróleo S/N
Prov. de Buenos Aires
Berisso, B1923
Argentina
<https://orcid.org/0000-0002-3940-987X>

Pablo César Favilla

Comisión Nacional de Energía Atómica
U.A.M. Div. Corrosión
Av. Gral. Paz 1499
Prov. de Buenos Aires
San Martín B1650KNA
Argentina
Pablo.Favilla@matthey.com

ABSTRACT: One of the characteristics of the synthesis of nanoparticles by reduction of

¹ Corresponding author. Tel.: +54 11 67727271. Fax.: +54 11 67727362.

precursor transition metals is the obtaining of a near monodispersize distribution, even when using different reducing agents, protective agents and conditions. A clear separation between the processes of nucleation and growth of nanoparticles is a necessary condition. This is true for mostly all of the nobler transition metals. The mechanism for different metals differs only in the relative values of the parameters, such as temperature, diffusion coefficients or kinetic constants that lead to the formation of the nanoparticles. The aim of this work is to present certain considerations about the mechanism showing the formation of nuclei is a consequence of the fluctuations in concentration during their formation. These are conditioned by the oxidation state of the metal, the reduction potential and the pH of the solution of synthesis. This work also demonstrates that the standard deviation for the final diameters is a consequence of the spatial distributions of nanoparticles in the solution during the growth and that there is a limit to the largest attainable specific area when using chemical methods.

KEYWORDS: Transition metals. Nanoparticles synthesis. Nucleation and growth mechanism. Thermodynamic properties. Low temperature fuel cells.

1 INTRODUCTION

In a series of works Finke *et al.* showed the first examples of welldefined compositional

synthesis for the formation of transition metal nanoparticles (NPs) by reduction of precursors. (Aiken et al., 1996; Besson et al., 2005; Hornstein et al., 2004; Özkar et al., 2002a, 2002b; Watzky et al., 2008, 1997; Widegren et al., 2001). The advantage of the Finke *et al.* technique is the monitoring of the total area of the NPs by the decrease in the pressure of hydrogen through the catalyzed reduction of the cyclohexene double bond on its surface.

These results show experimentally that the process is divided into two independent and consecutive steps in the case of systems in which NPs with a near monodispersesize distribution are obtained. Nuclei form in the first step, also called induction period (Özkar et al., 2002b; Watzky et al., 2008), in which no appreciable variation in hydrogen pressure is observed. The second or growth step evolves with a rapid increment of the electrochemically active surface, which results in a large variation in the hydrogen pressure owing to the catalytic effect of the metal. A remarkable fact of NPs synthesis by chemical reduction is that with different metal precursors, solvents, reducers and protective agents, a singularity is achieved: a nearmonodisperse material is always obtained. An example is the wide range of reducing agents that were used: gases such as hydrogen (Watzky et al., 2008, 1997), carbon monoxide (Kopple et al., 1980; Mucalo et al., 1989), formic acid method (H. Liu et al., 2006; Z. Liu et al., 2007; Prabhuram et al., 2003, 2004; Zhou et al., 2003), impregnation method followed by reduction with hydrogen at high temperature (H. Liu et al., 2006), oxidative solvents such as alcohols (Hirai et al., 1978; Roucoux et al., 2002), microwaveassisted polyol (Chu et al., 2010), polyol method (Acosta et al., 2017; Chen et al., 2005; Favilla et al., 2013; Oh et al., 2008; Yano et al., 2007), hydrides or salts such as sodium borohydride (A. B. R. Mayer et al., 1997; Andrea B. R. Mayer et al., 1997; Andrea B.R. Mayer, 1998; Andrea B R Mayer et al., 1998, 2000) or hydrazine, with similar results, i.e. nearmonodisperse NPs.

In order to avoid agglomeration of NPs, protective agents of steric or electrostatic nature can also be used. The steric stabilization is achieved by adding macromolecules such as oligomers and polymers (Evans, D.F., Wennerstrom, 1999; Everett, 1988; Hunter, 1987; Labib, 1988; Napper, 1983; Overbeek et al., 1981; Özkar et al., 2002a; Ross et al., 1988). In the case of the use of polyols as solvents and reducers, Polyvinylpyrrolidone PVP or carbonaceous supports are added, preventing the NPs mobility through the solution and thus hindering coalescence.

The electrostatic stabilization can be achieved using ionic solutions of compounds such as halides, polyoxoanions or carboxylates (Watzky et al., 2008, 1997). The adsorption of these compounds and their related counterions onto the metallic surface create an

electric doublelayer around the NPs generating electrostatic repulsion between them with the same results in all cases: agglomeration is avoided.

This behavior for different synthesis systems shows behind them kinetic and thermodynamic conditions or restrictions, which apply to all these systems. This is, however, only a final empirical consequence of the result. The questions that one asks are what the mechanism of nuclei formation is and what it depends on. The most direct speculation (based on classical chemical kinetics) is that the reducer reduces precursor atoms that then, by some diffusive mechanism, agglomerate to form nuclei. This mechanism is however highly unlikely because it is well known, that no matter how noble the metal is in the massive state, an isolated atom is totally unstable. The experimental measures for Ag (Belloni, 2002; Khatouri et al., 1993) show this instability quantitatively: the oxidation potential for an isolated silver atom is +1.8 V_{NHE} at pH 0. This potential makes the metal unstable in water, so a simple coalescence of independent atoms is highly improbable as a mechanism. The formation of nuclei obviously requires a much more complex process.

The aim of this work is to demonstrate that the nucleus formation mechanism is the same for all transition metals and is a consequence of concentration fluctuations that occur in this stage. We will show how this nucleation process depends on the oxidation state of the metal, the pH of the solution and the electrochemical potential of the reducer. We will explain why a standard deviation of the final diameters is generated, and what its relationship to the NPs concentration in the synthesis solution is.

The proposed mechanism works within a range of precursor concentrations called “thermodynamic limit”. The importance of this thermodynamic limit lies in the fact that these are the conditions for which the areas of NPs are the greatest possible that can be obtained from chemical synthesis.

This theory thermodynamically complements the phenomenological theory exposed by Richard Finke *et al.*, hence the title of this work.

2 FUNDAMENTAL

2.1 THE GENERAL EXPRESSION OF THE MEAN VOLUME AND SPECIFIC AREA

The mean volume of spherical NPs \bar{V}_{np} , synthesized by chemical methods starting with an initial concentration of precursor c_p^i , with a final Gaussian distribution of their diameters and with relative standard deviation α , is expressed by (Favilla et al., 2013):

$$\bar{V}_{np} = \frac{\pi}{6} \bar{d}^3 = \frac{MW}{(1 + 3\alpha^2)\rho_M} \frac{c_p^i}{\rho_{np}} = \frac{N_a a_0^3}{4(1 + 3\alpha^2)} \frac{c_p^i}{\rho_{np}} \quad (1)$$

where \bar{d} is the mean diameter of Nps, MW is the molecular weight of metal, ρ_M is the mass density of metal, ρ_{np} is the density of Nps per unit of volume of synthesis, N_a is the Avogadro's number and a_0 is the lattice parameter.

The expression of the specific area \bar{A} as a function of \bar{d} is, on the other hand, equal to the area of a NPs divided by the product of the density and volume, or:

$$\bar{A} = \bar{A}_{TEM} = \frac{6}{\rho_M} \frac{(1 + \alpha^2)}{(1 + 3\alpha^2)} \frac{1}{\bar{d}} \quad (2)$$

This specific area can be calculated using Transmission Electron Microscopy (TEM), measuring the diameter of the NPs and estimating their mean value \bar{d} and the relative standard deviation α . This specific area is hence called \bar{A}_{TEM} . Replacing the value of \bar{d} from Eq. (1) into Eq. (2), an expression for \bar{A}_{TEM} as a function of c_p^i , α and ρ_{np} is obtained:

$$\bar{A}_{TEM} = \frac{(1 + \alpha^2)}{(1 + 3\alpha^2)^{2/3}} \left(\frac{36 \pi}{MW \rho_M^2} \right)^{1/3} \left(\frac{\rho_{np}}{c_p^i} \right)^{1/3} \quad (3)$$

These expressions are as exact as precise are the measures of parameters they depend on. They are a consequence of a purely geometrical and statistical analysis of the final result of the synthesis. They carry no information on the mechanism itself.

One other thing to take into account is that the three parameters c_p^i , α and ρ_{np} , on which \bar{V}_{np} and \bar{A}_{TEM} , depend, do not have the same physical character. The value of c_p^i is defined by the experimenter before the test is started, while ρ_{np} and α are a consequence of the different processes taking place in the system. The constraints which are observed between these parameters is a consequence of the mechanism and its importance is hence clear.

The mechanical properties of a system (density, concentration, pressure, etc.) are defined from the point of view of statistical thermodynamics, as fluctuations around an average value, due to the corpuscular nature of matter. If the fluctuations are small, the system can be described neglecting them, taking into account only the mean value and its relationships with other mean values. There are however, systems with fluctuations of properties that become important, especially in those systems with complex and irreversible chemical reactions. Concentration fluctuations are the principal cause of the system evolution in the case of NPs synthesis by chemical methods. These fluctuations leave an irreversible and characteristic mark in the system, putting a final thermodynamic limit to the result.

2.2 THE DIAMETER DISTRIBUTIONS AND FLUCTUATIONS

In all synthesis of near monodispersesize NPs by chemical methods, the experimental final distribution of the diameters that define α is always Gaussian independently of the nature of the precursor or the reducer; it is neither the volume nor the mean area of the NPs. The explanation of this Gaussian distribution in the diameters is very simple and given by the growth mechanism. It is a consequence of the corpuscular character of matter, which is the same independently of the nature of the precursor or the reducer. From a phenomenological point of view, NPs growth rate v_g is completely controlled by precursor diffusion in the solution. Its change of mass m_M in time is proportional to the local concentration of the precursor at time t at \mathbf{r} and to the surface area of the NP (A_{np}), which allows us to write:

$$v_g = \frac{dm_M}{dt} = k_c A_{np}(t) c_p(\mathbf{r}, t) = k_c \pi d^2(t) c_p(\mathbf{r}, t) \quad (4)$$

the mass differential is on the other hand equal to:

$$\frac{dm_M}{dt} = \rho_M \frac{dV(t)}{dt} = \rho_M \frac{\pi}{2} d^2(t) \frac{dd(t)}{dt} \quad (5)$$

and by replacing Eq. (5) into Eq. (4) we obtain:

$$\frac{dd(t)}{dt} = \frac{2k_c}{\rho_M} c_p(\mathbf{r}, t) \quad (6)$$

This equation tells us that the variation in diameter during the growth process only depends on the concentration of precursor in the surroundings of the NPs. The concentration defined in Eq. (6), because of its corpuscular nature, is a mean value that suffers variations locally. Its value in different points of the system is a function of the local properties that are not necessarily uniform at that level. In Section 3.1 we will go back to revisit the issue.

2.3 THE KINETICS OF NUCLEATION

This section will demonstrate that the formation of nuclei is a consequence of the fluctuations in the concentration independently of the nature of the precursor and the reducer. The phenomenological mechanisms of the formation of nuclei and the mechanism corresponding to the growth process are of a different nature, even when both are consequences of the reduction of the metallic precursor.

Systems that present these two conditions during the synthesis: i) a clear separation between nucleation and growth processes, ii) an inhibition of NP agglomeration, show experimentally that the probability of forming a nucleus is proportional to the square root of the initial concentration of precursor and that the standard deviation of final diameters is proportional to the square root of ρ_{np} .

These two requisites are what we call the “thermodynamic limit”, i.e. the maximum specific area that can be obtained for that initial condition of synthesis. This requires a continuous environment of initial concentrations and constant conditions (pH, concentration of protective agents, etc.) for which the final resulting NPs mean volume and specific area can be predicted by evaluation of certain parameters of the system.

The close relationship between fluctuations in the concentration and the formation of nuclei was previously discussed. (Turkevich et al., 1953) It had already been speculate that the formation of clusters of several atoms of precursor having enough reduction energy and the necessary spatial distribution (precursor + reducer molecules, called embryos) would irreversibly evolve to a new state: the nucleus. In effect, this dependence of the reduction potential on the number of precursor atoms that form the clusters was experimentally measured for Ag. (Belloni, 2002; Khatouri et al., 1993) His experiments show that the oxidation potential of an isolated atom is $+1.8 V_{NHE}$. With the increase in the number of atoms in the clusters, the potential diminishes, being equal to $0.3 V_{NHE}$ for a cluster of 11 atoms (see Fig. 1 page 383 in Ref. (Belloni, 2002)). We deduce from the graph by Belloni *et al.* that any cluster made up of fewer than eight atoms will be unstable in water at pH=0. Embryos must have a minimum number of precursor atoms (critical number of atoms) to have a negative free energy of reduction that will allow the evolution of clusters into a nucleus.

What and how the structure of an embryo is, is unknown. All that matters is that once it is formed, it is very unstable and will collapse forming a nucleus. In these circumstances, the embryo has the necessary conditions to generate a massive electron exchange between the precursors and the molecules of reducer that form it. This would be a mechanism similar to the one Belloni *et al.* proposes to explain the reduction of grains of silver bromide in photographic films. (Belloni, 2002)(M. Mostafavi et al., 2002)

Fluctuations are events that occur repeatedly, that occur singly (only event to consider at that time) and independently, at instants of time that are random and with different intensities, which means they follow a Poisson statistics with uniform average rate occurrences per time unit. Those fluctuations strong enough to create an embryo with at least a critical number of atoms, or more, will have an average rate λ_N per volume

unit and will irreversibly react to become a nucleus. It is experimentally known that there is an induction time t_{ind} before NPs start their growth (i.e. a good separation between nucleation and growth processes). (Watzky et al., 1997) We can say that the value of λ_N equals the final number of NPs per volume unit divided by the induction time:

$$\lambda_N = \frac{\rho_{np}}{t_{ind}} \quad (7)$$

This process is characterized by its average rate λ_N , just as all Poisson processes are, but this tells us nothing about what those “positive” fluctuations depend on, those fluctuations strong enough to form a nucleus because of their thermodynamic conditions.

The concentration fluctuations in the solution at a given point \mathbf{r} are expressed by the difference:

$$\delta c_p(\mathbf{r}) = c_p(\mathbf{r}) - c_p^i \quad (8)$$

These fluctuations will be centered around c_p^i and their standard deviation will be equal to: (Keizer, 1982, 1987a, 1987b; Landau et al., 1988; Molski, 1996)

$$\sigma_c = \sqrt{\langle \delta c_p(\mathbf{r}) \delta c_p(\mathbf{r}') \rangle} \approx (c_p^i)^{1/2} \delta_D(\mathbf{r} - \mathbf{r}') \quad (9)$$

“Positive” fluctuations will therefore be proportional to σ_c giving an amount of formed nuclei per unit of volume ρ_{np} proportional to σ_c , allowing us to write;

$$\rho_{np} = k_{np} (c_p^i)^{1/2} \quad (10)$$

the parameter k_{np} being a constant that depends on the properties of the synthesis system in question. We must consider that during induction time, the concentration of the formed nuclei, consisting of a few atoms, is several orders of magnitude smaller than the precursor concentration. It can thus be considered that during nucleation, the precursor concentration is always equal to c_p^i .

Introducing Eq. (10) into (1) we obtain expression:

$$\bar{V} = \frac{\pi}{6} \bar{d}^3 = \frac{MW}{(1 + 3\alpha^2)\rho_M k_{np}} (c_p^i)^{1/2} = \frac{N_a a_0^3}{4(1 + 3\alpha^2) k_{np}} (c_p^i)^{1/2} \quad (11)$$

The verification of this relationship is a necessary and sufficient condition for the system to be in the thermodynamic limit.

3 EXPERIMENTAL

The NPs were prepared using the modified polyol method.(Chen et al., 2005) The precursor was Platinum (VI) H_2PtCl_6 , Palladium (II) $PdCl_2$ and Rhodium (III) $RhCl_3$. The solvent and reducing agent was an ethylene glycolwater solution (volume ratio 3:1). Catalysts were prepared with a protecting agent PVP to prevent aggregation of NPs. The amount of PVP added to the solution was measure in relation to metal quantity, the molar ratio used was PVP/metal 0.1 (referred to monomer unit of PVP). The support for all catalysts was carbon black powder (Vulcan XC72R, Cabot international) with area BET $250\text{ m}^2\text{ g}^{-1}$, in general added before begging the synthesis. Taking into account the precursor initial concentration, the amount of Vulcan XC72R is the necessary to obtain X% metal nominal loads (define as the weight percentage of metal in the catalyst consisting of metal and carbon).

Different studies of the variation of mean volume with different initial concentrations of precursor done by us for Pt, Pd and Rh are presented in this section.

Figure 1 shows the results obtained for the synthesis of Pd NPs at pH 12 in Ref. (Acosta et al., 2017) and pH 6 which follow Eq. (11). For the case of the synthesis at pH 12 and from the slope between 0.5 and 6 mM, a value for k_{np} of $3.71\pm 0,06)10^{17}$ Part. moles $^{-1/2}\text{ cm}^{2/3}$ was calculated. At values of c_p^i below 0.5 mM there is a deviation from this behavior. The increase in the mean volume means a decrease in the value of ρ_{np} with respect to the one predicted by Eq. (10) which is caused by a not so net separation between nucleation and growth processes. We discuss this at the end of Section 3.3.

In the case of the synthesis at pH 6, a good correlation is observed. A k_{np} of $2.5\pm 0,1)10^{17}$ Part.moles $^{-1/2}\text{ cm}^{2/3}$ was calculated.

Fig. 1. Relationship between the mean volume of Pd NPs and $(c_p^i)^{1/2}$ (initial pH for synthesis: pH 12 and pH 6). Red dots mark the data that are away from the thermodynamic limit.

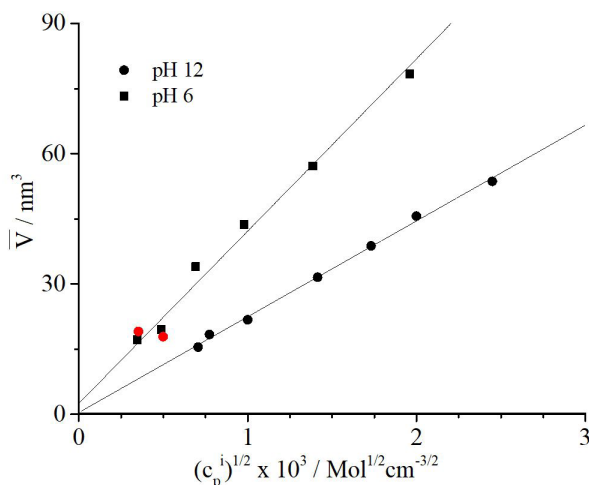


Figure 2 shows the results obtained for Rh NPs synthesis at an acid pH. A good correlation is observed up to 1.6 mM, which validates Eq. (11). The value at 3.6 mM shows an increase in the mean value (65.4 nm^3) with respect to the one that the equation predicts (40.8 nm^3). This difference can be attributed to an important coalescence of nuclei during nucleation which reduces the final number of NPs and the value of ρ_{np} . We discuss this at the end of section 3.3 as well. The value for k_{np} in Rh obtained from the slope is $4.5 \pm 0.3)10^{17} \text{ Part. mol}^{-1/2} \text{ cm}^{2/3}$.

Figure 3 shows the results obtained for Pt NPs synthesis at an acid pH. This graph also shows a linear correlation for c_p^i values below 2 mM, which is again in accordance with Eq. (11). As is the case for Rh, values above 2 mM show the nuclei coalescence during nucleation and a sharp decrease in the value of ρ_{np} . An experimental value for k_{np} below 2 mM is obtained from the slope that equals $8.5 \pm 0.5)10^{17} \text{ Part. mol}^{-1/2} \text{ cm}^{2/3}$.

Fig. 2. Relationship between the mean volume of Rh NPs and $(c_p^i)^{1/2}$. The red dot marks a datum that is away from the thermodynamic limit.

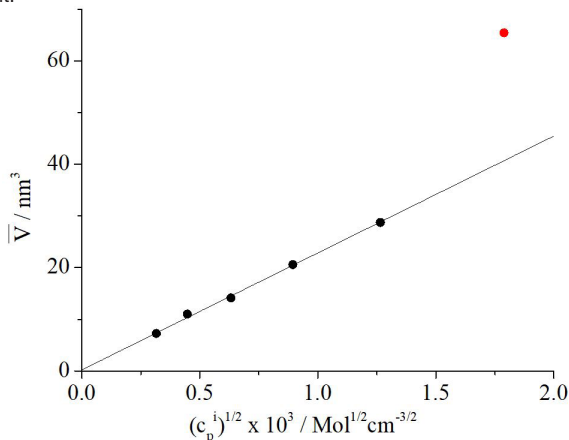


Fig. 3. Relationship between the mean volume of Pt NPs and $(c_p^i)^{1/2}$.

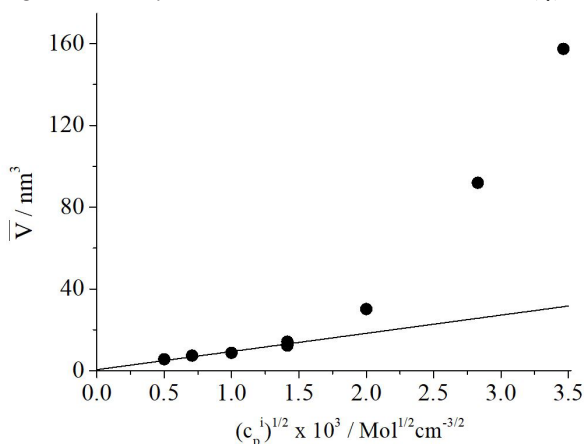
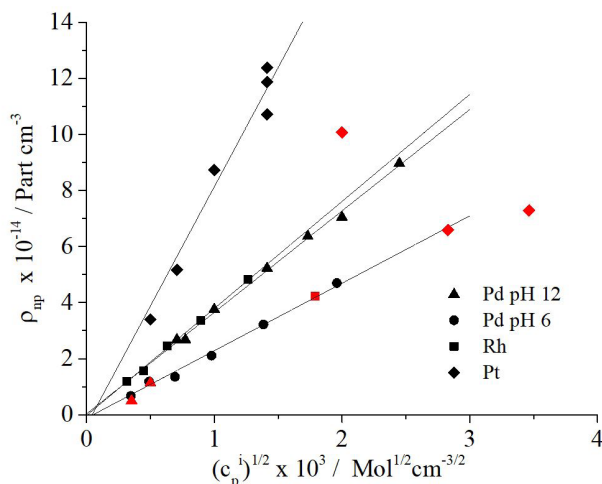


Figure 4 depicts a graph of ρ_{np} as a function of $(c_p^i)^{1/2}$. The values of ρ_{np} were obtained applying Eq. (1) from the calculated values of \bar{v}_{np} and α obtained from the histograms of the diameter distribution. Results show a linear proportionality within the limits of the thermodynamic limit as is predicted by Eq. (10). The value ρ_{np} for all tests outside this limit is always inferior to the one Eq. (10) predicts (i.e. see red points in Fig. 4).

Fig. 4. NPs density in solution as a function of $(c_p^i)^{1/2}$. Red dots mark the data that are away from the thermodynamic limit.



3.1 THE RELATIONSHIP BETWEEN THE STANDARD DEVIATION OF THE FINAL DIAMETER σ_d AND ρ_{np}

In Section 2.2 we showed that the experimental final distribution of the diameters is always Gaussian independently of both the precursor and the reducer nature. Equation (6) predicts that the variation of the diameter during growth is only a function of the local concentration of the precursor. As Finke *et al.* demonstrated, growth involves a fast surface autocatalytic reaction and is therefore completely controlled by diffusion of the precursor towards the NP. (Aiken *et al.*, 1996; Besson *et al.*, 2005; Hornstein *et al.*, 2004; Özkar *et al.*, 2002a, 2002b; Watzky *et al.*, 2008, 1997; Widegren *et al.*, 2001) If NPs were homogeneously distributed in the solution they would be indistinguishable, each NP having the same environment. In this hypothetical case, the observer would see that at the end of the synthesis all NPs would have the same diameter. The value of ρ_{np} is a mean value, as is c_p^i which means that there exists a local variation $\rho_{np}(\mathbf{r})$ due to its corpuscular character. These local variations are very small and can be considered as independent from each other. This explains why the distribution function for the probability of measuring a given local concentration is Gaussian and centered round the mean value ρ_{np} .

The dispersion of this distribution can be characterized completely using the standard deviation σ_p (Landau et al., 1988) that equals:

$$\sigma_p = \sqrt{\langle \delta \rho_{np}(\mathbf{r}) \delta \rho_{np}(\mathbf{r}') \rangle} \approx (\rho_{np})^{1/2} \delta_D(\mathbf{r}-\mathbf{r}') \quad (12)$$

where δ_D is an impulsive function or Dirac's delta. We developed a qualitative explanation for this mechanism in Ref. (Acosta et al., 2017).

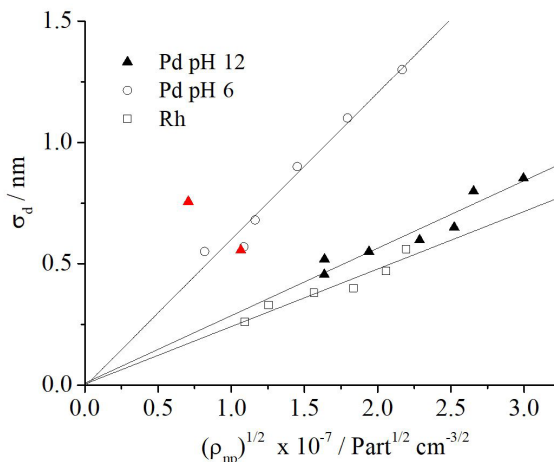
Given that the standard deviation of the diameters σ_d depends only on the local concentration of the precursor in the neighborhood of the NPs, that this concentration depends on the spatial distributions of NPs in the solution and that both distributions are Gaussian, we have that σ_d is proportional to σ_p . So using Eq. (12) we obtain:

$$\sigma_d = k_\sigma (\rho_{np})^{1/2} \quad (13)$$

Figure 5 shows the graph of values of σ_d obtained from the analysis of TEM micrographs versus the square root of ρ_{np} . Data obtained on Pt in the zone of the thermodynamic limit (i.e. below to 2 mM) have not been shown since the values of σ_d are practically independent from ρ_{np} , and NPs are much more numerous than in the other metal cases studied, making it difficult to determine their number because of the superimposition of NPs in the TEM micrographs.

Although we observe dispersions, the three cases in the graph show a good correlation and verify Eq. (13). Data, although there are different slopes, tend to converge to the origin, as this equation predicted.

Fig. 5. Standard deviation of the diameters as a function of the square root of the density of NPs. Red points show data that are away from the thermodynamic limit.



The following values of k_g were obtained from the slopes of the curves in Fig. 5: $6.1 \pm 0.5)10^{-8}$ for Pd at pH 6, $2.8 \pm 0.2)10^{-8}$ for Pd at pH 12 and $2.4 \pm 0.2)10^{-8}$ for Rh in acid media (in Part: $^{-1/2} \text{ nm cm}^{3/2}$).

3.2 ON THE SIZE OF THE NUCLEI AND THE NUCLEATION RATE

The experimental results of Belloni *et al.* for Ag (Belloni, 2002; Khatouri et al., 1993) show that the smaller the amount of atoms in a nucleus, the lesser noble the metal is. There is a minimum number of atoms, below which nuclei are unstable. This thermodynamic consideration allows us to define a critical or thermodynamic number of atoms over which nuclei are stable.

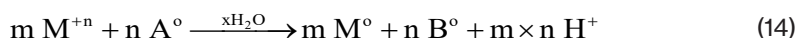
Considering the validity of the microreversibility principle or detailed equilibrium (De Groot et al., 1984) but from the point of view of the genesis or formation of nuclei, no nucleus will form unless the embryo formed during the fluctuation contains this minimum number of atoms.

From the electrochemical point of view, this number of atoms above which nuclei are stable also depends on the oxidation potential of the reducer. It can be stated from the chemical instability of the process or its spontaneity (i.e. GibbsDuhem $\Delta G_{T,P} < 0$) that any embryos that have this number of atoms or more, are thermodynamically unstable and irreversibly become nuclei. This concept is what defines the critical formation diameter in this type of nucleation.

La Mer and Dinegar's model for the formation of colloids in over saturated solution states that the critical diameter surges from a compromise between the surface energy, depending on the area, and the value of the free energy of formation of a nucleus, depending on the embryo volume. (LaMer et al., 1950) It has been nevertheless shown that when nuclei are formed by reduction of transition metals, the critical diameter depends on the free energy for reduction in the cluster. The processes are different, hence different concepts of critical diameters in both cases.

If the precursor solution has its temperature and pressure well below the values for synthesis, the system is in a nonequilibrium state. Its kinetics is very slow because those concentration fluctuations that can lead to nuclei formation are negligible. At the temperature for synthesis, the frequency of the fluctuations become high enough to irreversibly take the system to the final state.

The global reaction of this process can be written as:



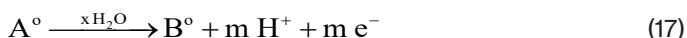
We have to take into account that the initial process (precursor + reducer solvent) is far from equilibrium, so the initial rate of the chemical reaction v does not depend on its chemical affinity (Glansdorff et al., 1971) and is:

$$v = \bar{k} a_{M^{n+}}^m a_{A^0}^n \quad (15)$$

This condition makes it impossible to define a thermodynamic potential for the initial process, but it is possible to define a local thermodynamic potential in which the Gibbs equation based on the local equilibrium hypothesis is assumed to be valid for each volume differential. This is the fundamental hypothesis on which all the theory of irreversible processes is based. Next, a generic expression of ΔG for the formation of a metallic nucleus will be given, taking into account the oxidoreduction reactions for a system close to equilibrium and that as the ΔG is an extensive property, the expression will be valid in a point or spatial volume differential. We thus have in generic form for the reduction of the metal, that:



This reduction is associated with the oxidation of the reducer that can be either added externally or, in the case of alcohols and polyols, is the solvent itself, so in general it can be written that:



It has been here assumed that the solvent (compound A^0) also fulfills the function of a reducer decomposing into another compound B^0 that in turn generates protons to the medium consuming water. In the case of ethylene glycol, A^0 is the ethylene glycol and B^0 the glycolic or oxalic acid. This reaction is very general, for example, the reducer might not consume water and its reaction might be independent of the pH, as for example the couples, Sn^{+2}/Sn^{+4} and Ce^{+3}/Ce^{+4} , or producing well reducing free radicals by radiolysis with γ rays. (Mehran Mostafavi et al., 1990; Torigoe et al., 2002)

Considering these two hemi reactions, ΔG equals:

$$\Delta G = -n \times m F (E_{red}^{M^{+n}/M^0} - E_{red}^{A^0/B^0}) \quad (18)$$

where F is the Faraday constant and,

$$E_{\text{red}}^{M^{+n}/M^0} = E_{\text{red},M} - \frac{RT}{nF} \ln \frac{a_{M^0}}{a_{M^{+n}}} \quad (19)$$

$$E_{\text{red}}^{B^0/A^0} = E_{\text{red},B} - \frac{RT}{mF} \ln \frac{a_{A^0}}{a_{B^0} (a_{H^+})^m} \quad (20)$$

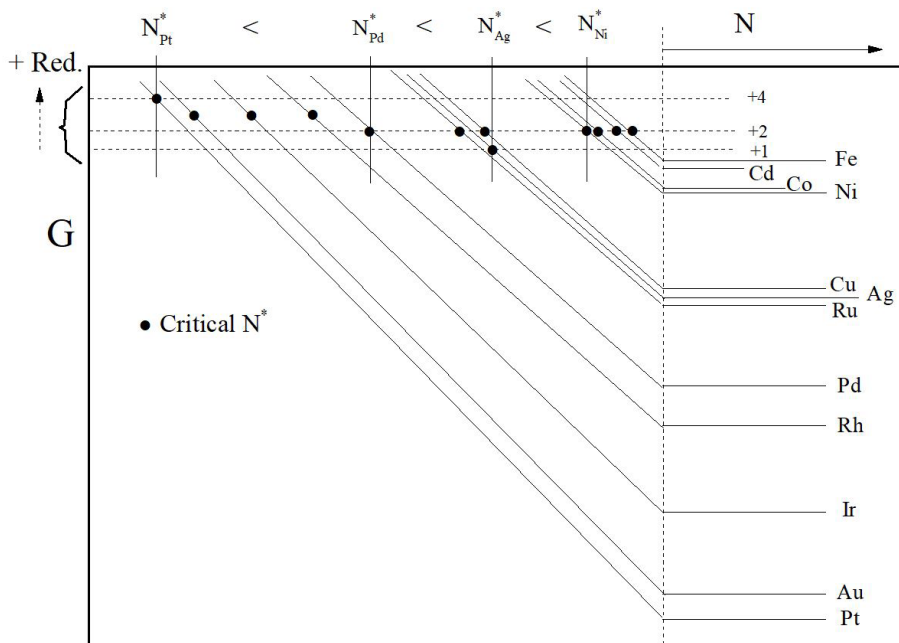
Introducing these two last equations into Eq. (18) and ordering the final expression we obtain that:

$$\Delta G = \Delta G^0 - n \times m \cdot 2.303 RT \text{ pH} + RT \ln \frac{(a_{B^0})^n}{(a_{A^0})^n} + RT \ln \frac{(a_{M^0})^m}{(a_{M^{+n}})^m} \quad (21)$$

Figure 6 shows a schematic representation of the free energy for different metals as a function of the number of atoms N that constitute the nucleus. For a given metal and value of N, the ΔG of these nucleus equals the difference between the free energies defined by the full line for N and the one given by the horizontal dotted lines, each depending on the oxidation number of the metallic precursor, on the electrical potential of the reducing agent and in certain cases, on the pH.

The ΔG can be divided into four terms. Considering one predetermined reducing agent, the first term of Eq. (21) is always a negative value (i.e. the nobler the metal, the more negative it is). The second term takes into account the pH of the solution and is related to the electrical potential of the reducer if it generates protons during the reaction; it is more negative the higher the pH. In this case the basic pH favors the reaction. The third term is the relationship between the activities of the oxidized and reduced species of the reducer and can be considered almost constant given the high concentration of the solvent a_{A^0} in the embryo and the amount of oxidized product a_{B^0} . This share is considered in the dotted lines in Fig. 6. The position of the dotted stripes depends on the reducing power of the reducer and on the pH; they are more positive the higher the reducing power and the higher the pH (this effect is symbolized in Fig. 6 by the dotted arrow in the upper left margin). The last term is the relationship between the activities of the metal in solution and the concentration of the precursor. It depends on the concentration of atoms of the precursor that constitute fluctuation $a_{M^{+n}}$ and on the activity of the solid a_{M^0} that is highly dependent on the critical number of atoms in the nucleus. The oblique lines in the scheme in Fig. 6 represent this variation.

Fig. 6. Scheme of the variation in free energy as a function of the amount of atoms that constitute the NPs for different metals. ● Values of the critical N^* for different metals and for the same reducer (horizontal dotted line).



All solutions with embryos produced by the fluctuation with N number of atoms of precursor above the black dots in Fig. 6 will have $\Delta G > 0$ and will therefore not transform into metallic nuclei. On the contrary, all those embryos with N precursor atoms that have $\Delta G < 0$ will be unstable and transform spontaneously into metallic nuclei.

The black dots correspond to the number of atoms in the minimum embryo (N^*) that are required to have a negative value for ΔG , i.e. the critical N^* .

The variation of the free energy of the metal with the number of atoms of the embryo N in the scheme (that is, the oblique lines), is an approximate value given that the exact variation in the free energy as a function of the number of atoms of the NP is unknown. This approach is good enough to justify, however, many of the experimental facts observed in the synthesis of NPs about the size of nuclei and their rate of formation. Belloni's data for Ag show a relationship between the electric potential (a relative measure of the free energy) and the number N , very similar to those in Fig. 6. See Fig. 1 page 383 in Ref. (Belloni, 2002).

Experiment show, there is an inverse relationship between the rate of nucleation and the critical size of nuclei. The smaller the critical number of atoms N^* for the formation of the nucleus the more likely it is to form, thus increasing the rate of nucleation which

ultimately translates into an increase in the final density of NPs in solution. So metals that have statistically large values of N^* will form fewer nuclei during the induction time and will increase their diameters during the growth process (i.e. for the same initial concentration there will be fewer nuclei to share what is left of the precursor in solution).

Some useful concepts follow from the energetic scheme in Fig. 6, which are useful to interpret the experimental data observed for certain precursor:

- The nobler the metal, the smaller N^* tends to be.
- When the reducer produces protons, as is the case with polyols, nuclei will be smaller the higher the oxidation number of the precursor and the amount of protons produced in the reduction.
- For the same conditions, if the reducer produces protons, basic media will yield smaller NPs.

This model predicts several results present in literature, as the following examples show. We find that noble metals such as Au, Pt and Ir usually form high density nanometric colloids very easily, made up of monodisperse NPs with mean diameters between 1 and 4 nm. (Favilla et al., 2013; B. H. Kim et al., 2014) It is well known how simple it is to make nanometric colloids of Au. (Luo, 2007; Peng et al., 2008; Turkevich et al., 1951, 1953)

The data reported on Table 1 in Ref. (Watzky et al., 2008), show a very close value in the mean diameter (i.e. 2.1 nm) for nine synthesis of Ir NPs with different precursors. This shows that within the experimental error ρ_{np} is similar in their nine synthesis using different precursors but the same reducer and c_p^i (i.e. 1.2 mM). The formation of nuclei does not depend on the initial chemical composition of the precursor or on the metal complexes it might form in the solution.

The synthesis of Ag NPs using $AgNO_3$ as the precursor yields NPs that are much bigger than the ones obtained for Pd under same conditions and with greater a dispersion in their diameters as well. In this case the oxidation number of the metal is I, the mean diameters obtained are of 1750 nm. (Hei et al., 2010; D. Kim et al., 2006; Yan et al., 2011)

In the work by Zhao *et al.*, the synthesis were carried out at pH 10 by the addition of ammonia, in order to obtain smaller mean diameters. The argument given by the authors is that complex $Ag(NH_3)_2^+$ is more difficult to reduce than Ag^+ . (Hei et al., 2010) This argument is contrary to the theory stated in this work because, if the complex were more difficult to reduce, NPs would have a bigger mean diameter given that, statistically, fewer nuclei would form. As previously noted, the measurements by Finke *et al.* in Ir (Watzky et al., 2008) show that the formation of nuclei is independent of any possible metal complexes in

the synthesis solution. The experiment shows how important the solution pH is: ammonia is a base that increases the initial pH.

The results for Pd at different pH values in Ref. (Acosta et al., 2017) clearly show that NPs are much smaller in a basic medium (≈ 4 nm) than in an acidic medium (≈ 18 nm).

Ionizing radiation generates free radicals that are very reducing and allow the formation of very small aggregates that are not formed by conventional chemical methods. In the case of Ag, the data obtained by Belloni *et al.* by γ -irradiation of solutions containing Ag and polyacrylate ions are conclusive, with the formation of aggregates of less than ten atoms stabilized by the polyacrylate. (Mehran Mostafavi et al., 1990)

One other interesting experiment result that matches this theory is the synthesis of NPs with Rh and Ag in the same solution. (Torigoe et al., 2002) In the case of these two metals no alloys are formed, fact that is explained by considering the big difference in the lattice parameters they have. It has also been observed that the ions of Rh do not adsorb on the aggregates of Ag and vice versa. Rh and Ag form isolated pure aggregates. This experiment yielded pure Ag NPs of diameters between 15 and 20 nm with a smaller NP density than Rh, which had a mean diameter of 1.52 nm, result that matches qualitatively what the diagram in Fig. 6 predicts.

In the case of syntheses by the polyol method for Ni and Co NPs, Fievet *et al.* obtain NPs larger than a micron. When they add a precursor in low concentrations such as Ag or Pd, to attain heterogeneous nucleation, they obtain NPs smaller than the micron and monodisperse. (Fievet et al., 1989) The explanation is that Ag and Pd form many more nuclei that will grow from the metal (i.e. core-shell type growth).

In the case of Cu, using polyol method in the presence of PVP, Park *et al.* obtain 45 nm in diameter NPs (Park et al., 2007), similar in size to those obtained with Ag (Hei et al., 2010; D. Kim et al., 2006; Yan et al., 2011), as the diagram in Fig. 6 predicts. With an increase in the reducing power of the solution, the synthesis of Cu NPs with NaBH_4 in presence of PVP produced NPs of a mean diameter of 7 nm. (Aguilar et al., 2019) Silver, nobler than Cu, should generate smaller NPs, but this effect is compensated by the influence of the oxidation state of the precursor, II for Cu and I for Ag, thus generating NPs of similar mean diameter (see Fig. 6).

Bibliography shows the difficulty that exists for the syntheses of NPs in Ni. This is in accordance with what this work predicts in Fig. 6 for the value of N_{Ni}^* . Couto *et al.* made tests starting from NiCl_2 dissolved in ethylene glycol. (Couto et al., 2007) They observed no formation of NPs in these conditions, even when they carried out the reaction at a high temperature. When they added NaBH_4 they obtained NPs with mean diameters

between 3.47.7 nm depending on the amounts of PVP added. Wu and Chen obtained Ni monodispersed NPs of a mean diameter of 9.2 nm without protective agent, through the hydrazine reduction of NiCl₂ in ethylene glycol in the presence of appropriate amounts of NaOH. (Wu et al., 2003) The reducing power of NaBH₄ is well known and is higher than that of hydrazine. Great quantity of nuclei form in this case because the reduction potential of the reducer is strongly augmented. This is equivalent to increasing the value of the dotted lines in Fig. 6. The stronger the reducing power, the smaller the NPs (3.47.7 nm with NaBH₄ and 9.2 nm with hydrazine). These results match what Blossi *et al.* obtained when synthesizing Ni NPs in ethylene glycol with PVP and dodecylamine (DDA) as steric protectors by heating in a microwave oven to get NPs with final diameters larger than 80 nm. (Blossi et al., 2013)

This theory explains why it is important that the electrical reducing potential be high, because it increases the probability of nucleus formation and hence, the nucleation rate during induction time. It also shows there is a compromise between the specific area and the corrosion of NPs. The smaller the NPs the easier they oxidize and the more unstable the catalyst results. This is one of the problems present in fuel cells when their durability is concerned and sets a limit to the maximum specific area for each metal in particular.

3.3 ELECTROCHEMICAL MEASURES OF THE SURFACE AREA

We can obtain an expression for the specific area by combining Eq. (3) with Eq. (10), in the zone of the thermodynamic limit, which is independent of the final density of NPs in solution, so:

$$\bar{A}_{\text{TEM}} = \frac{(1 + \alpha^2)}{(1 + 3\alpha^2)^{2/3}} \left(\frac{36 \pi k_{\text{np}}}{\text{MW } \rho_{\text{M}}^2} \right)^{1/3} (c_{\text{p}}^i)^{-1/6} \quad (22)$$

Given that in the thermodynamic limit, α factor is quasi constant and that the other parameters are intrinsic parameters for the metal and the method, the specific area only depends on $(c_{\text{p}}^i)^{-1/6}$. This expression allows us to relate the electrochemical area (from the voltogram peaks) and the physical characteristics obtained from TEM micrographs. The electrochemical surface area ECSA is determined from area Q^{X} in CVs⁻¹ of the adsorbed species “X” in the voltogram peak, taking the current of the electric doublelayer as the base line and using equation:

$$\text{ECSA} = \frac{Q^{\text{X}}}{n \Gamma^{\circ} v_s m_{\text{M}}} \quad (23)$$

where Γ° is the specific charge of a monolayer of adsorbed atoms ($210 \mu\text{C cm}^{-2}$), n the number of electrons exchanged per adsorbed atom, v_s the sweep rate and m_M the total mass of metal deposited on the electrode (see (Acosta et al., 2017)). The value of ECSA is proportional to the real electrode area and can be measured by three different methods: a) hydrogen desorption/adsorption peaks, b) metal oxidation peak and c) previously adsorbed carbon monoxide oxidation peak. Three electrochemical efficiency factors for the area are defined from these methods $\eta_A^{\text{H}_2}$, η_A^{Ox} and η_A^{CO} , respectively, the superscripts referring to the electrochemical area measurement method used. This factor is defined as the quotient between the specific area calculated electrochemically by a given method and the \bar{A}_{TEM} , that is:

$$\text{ECSA} = \eta_A^X \bar{A}_{\text{TEM}} = \eta_A^X \frac{(1 + \alpha^2)}{(1 + 3\alpha^2)^{2/3}} \left(\frac{36 \pi k_{\text{np}}}{\text{MW } \rho_M^2} \right)^{1/3} (c_P^i)^{-1/6} \quad (24)$$

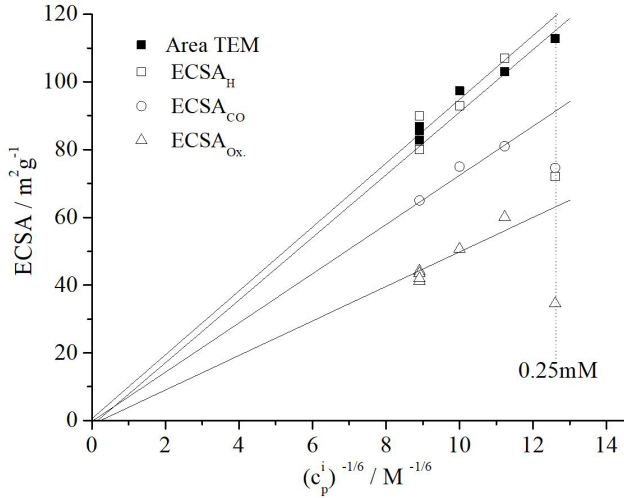
The area efficiency factor η_A^X has two different contributions: i) the profitability factor of the catalyst area ϕ that is related to the useful part of the catalyst and ii) the value of the surface coverage of the adsorbed species "X", θ^X , that depends on the nature of the interaction adsorbate/metal. It is equal to the quotient between the detected charge Q^X and the monolayer charge (equal to the number of exchanged electrons per adsorbate molecule, i.e. one for hydrogen and two for oxygen and carbon monoxide, multiplied by Γ°), this is:

$$\eta_A^X = \phi \theta^X \quad (25)$$

Factor ϕ is independent of the adsorbate nature and takes into account the loss of real electroactive area of the NPs, as for example: NPs with no electrical contact to the carbonous support or parts of the catalyst area blocked by the adsorbed carbon grain. A value of one corresponds to a total use of NPs area.

Figures 7 and 8 show the calculations for ECSA in the cases of Pt and Rh and the peaks of hydrogen, oxygen and carbon monoxide desorption as a function of $(c_P^i)^{-1/6}$, for data within the thermodynamic limit. All cases show a proportional linear regression.

Fig 7. Variation of ECSA for Pt calculated by different methods with $(c_p^i)^{-1/6}$.



The quotient between the \bar{A}_{TEM} slope and the other slopes (from Figs. 7 and 8) yielded the value of the area efficiency factors for Pt and Rh. The value of η_A^{Ox} calculated from the peak of oxygen reduction matches a type α (2x2) structure ($\theta^{Ox} = 0.50$). (Todorova et al., 2003) The value of η_A^{CO} obtained from the peak for the reduction of CO is consistent with a type α (2x2)-3CO structure ($\theta^{CO} = 0.75$). (Rupprechter et al., 2004) The values of η_A^H from the hydrogen peak are consistent with a α (1x1) structure ($\theta^H = 1$) for Pt and Rh. The values of η_A^{Ox} and η_A^{CO} from Fig. 9 for Pd at pH 6 were also calculated. Table 1 shows a summary of the different area efficiency factors for all studied cases plus data for Pd at pH 12 from Acosta *et al.* (Acosta et al., 2017)

Fig. 8. Variation of ECSA for Rh calculated by different methods with $(c_p^i)^{-1/6}$.

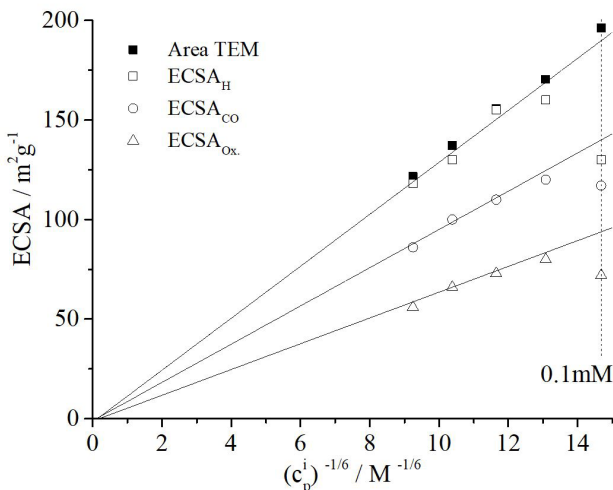


Fig. 9. Variation of ECSA for Pd at pH 6 calculated by different methods with $(c_p^i)^{-1/6}$.

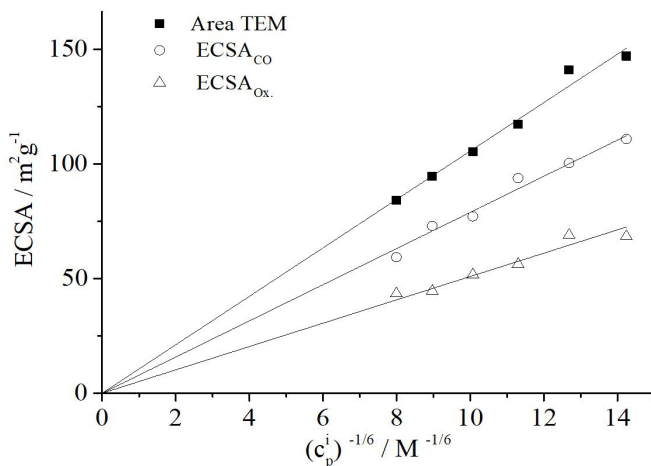


Table 1. Values of area efficiency factors obtained for the three different metals studied.

	Pt	Rh	Pd at pH 6	Pd at pH 12 in (Acosta et al., 2017)
$\eta_A^{H_2}$	0.98	0.95	--	--
η_A^{Ox}	0.54	0.47	0.48	0.51
η_A^{CO}	0.77	0.72	0.75	0.71

A value close to one for ϕ can be assumed for the three cases, considering the error in values of η_A^x , that are less than 5%. An important decrease in ECSA for the value of c_p^i for Pt of 0.25 mM (Fig. 7) and for Rh 0.1 mM (Fig. 8), is observed. The value of \bar{A}_{TEM} is nevertheless consistent with the area that Eq. (22) predicts because in Pt and Rh the nucleation and growth processes are well separated. It seems that the smaller value of ECSA is a consequence of a diminished catalytic activity because of a high decrease in the mean diameter. This is an effect that is important in the production of fuel cell catalyzers.

In the case of Pd, on the contrary, this decrease is observed in both ECSA and \bar{A}_{TEM} . (Acosta et al., 2017) The decrease in the case of Pd of the value of \bar{A}_{TEM} is a consequence of the loss of a neat separation between the nucleation and growth processes.

4 CONCLUSION

Several concepts and conclusions can be drawn from the syntheses of NPs for transition metals:

- We demonstrated that for a given initial synthesis condition and for various metals, that there is a zone we call the “thermodynamic limit” and this just by modifying the initial concentration of the precursor. In this zone there are certain constraints that allow the obtaining of a maximum specific area for that particular initial synthesis condition.
- We showed that the number of nuclei is a consequence of the fluctuations in concentration through a mechanism of formation of embryos having a critical number of atoms of precursor that makes the system unstable and forces the irreversible transformation of the embryos into a metallic nucleus. The smaller the critical number of atoms for the formation of a nucleus, the more probable its irreversible transformation is, fact which increases the rate of nucleation, which finally translates into a higher final density of NPs. The critical number depends on the electrical reducing potential of the metal, on its oxidation state, on the pH of the solution and on the potential of the reducer. The NPs density in solution is proportional to the square root of the initial concentration of precursor.
- The final standard deviation in the diameters is a consequence of the local concentration of the precursor in the neighborhood of the NPs; this concentration depends on the distribution of the NPs in the solution. This last point turns the standard deviation in the final diameters into a consequence of the spatial distributions of the nuclei concentration, which is therefore proportional to the square root of the density of NPs in solution.
- For the same initial concentration of precursor, the mean diameter depends on the initial pH of the synthesis and is higher for low values of pH. Alkaline pHs enhance the nucleation process by increasing its rate.
- The mean diameter, its standard deviation, the mean volume and the specific area of NPs can be predicted for a given metal and for any initial concentration of precursor, if the values of k_{np} and k_{σ} are known. This is true within the thermodynamic limit and with equal synthesis conditions (i.e. same reducers and protective agents)
- Within the thermodynamic limit zone, the proportionality factors between the areas calculated using the mean diameters \overline{A}_{TEM} and the electrochemical areas ECSA, are constant.

- For the adsorption of oxygen and carbon monoxide on a catalyst surface, experimental results are consistent with a type α (2×2) structure ($\theta^{\text{ox}} = 0.50$) and β (2×2)-3CO structure ($\theta^{\text{co}} = 0.75$), respectively. In Pt and Rh adsorption of hydrogen is consistent with a β (1×1) structure ($\theta^{\text{H}} = 1$). The value of the factor ϕ , which takes into account the loss in electro active specific area, is close to one, within the experimental error, proving that all the area of the catalyst is being used in Vulcan XC72R as support.

5 ACKNOWLEDGMENTS

This work was financially supported by: Dpto. Materiales del Centro Atómico Constituyentes de la Comisión Nacional de Energía Atómica (UAMCACCNEA). The authors would like to especially thank R.E. Gonnet for her remarks concerning several parts in this paper.

REFERENCES

- Acosta, J. J., Favilla, P. C., & Collet-Lacoste, J. R. (2017). Chemical Synthesis and Characterization of Carbon Supported Palladium Electro-Catalysts. *International Journal of Nanoscience*, 15(4), 1750007. doi: 10.1142/S0219581X17500077
- Aguilar, M. S., Esparza, R., & Rosas, G. (2019). Synthesis of Cu nanoparticles by chemical reduction method. *Transactions of Nonferrous Metals Society of China*, 29(7), 1510–1515. doi: 10.1016/S1003-6326(19)65058-2
- Aiken, J. D., Lin, Y., & Finke, R. G. (1996). A perspective on noncluster catalysis: Polyoxoanion and (n-C₄H₉)₄N⁺ stabilized Ir(O)(-300) nanocluster “soluble heterogeneous catalysts.” *Journal of Molecular Catalysis A: Chemical*, 114(1–3), 29–51. doi: 10.1016/S1381-1169(96)00302-0
- Belloni, J. (2002). The role of silver clusters in photography. *Comptes Rendus Physique*, 3(3), 381–390. doi: 10.1016/S1631-0705(02)01321-X
- Besson, C., Finney, E. E., & Finke, R. G. (2005). A mechanism for transition-metal nanoparticle self-assembly. *Journal of the American Chemical Society*, 127(22), 8179–8184. doi: 10.1021/ja0504439
- Blosi, M., Albonetti, S., Costa, A. L., Sangiorgi, N., & Sanson, A. (2013). Easily scalable synthesis of Ni nanosols suitable for the hydrogenation of 4-nitrophenol to p-aminophenol under mild condition. *Chemical Engineering Journal*, 215–216, 616–625. doi: 10.1016/j.cej.2012.11.013
- Chen, M., & Xing, Y. (2005). Polymer-mediated synthesis of highly dispersed Pt nanoparticles on carbon black. *Langmuir*, 21(20), 9334–9338. doi: 10.1021/la051892p
- Chu, Y.-Y., Wang, Z.-B., Gu, D.-M., & Yin, G.-P. (2010). Performance of Pt/C catalysts prepared by microwave-assisted polyol process for methanol electrooxidation. *Journal of Power Sources*, 195(7), 1799–1804. doi: 10.1016/j.jpowsour.2009.10.039
- Couto, G. G., Klein, J. J., Schreiner, W. H., Mosca, D. H., de Oliveira, A. J. a., & Zarkin, A. J. G. (2007). Nickel nanoparticles obtained by a modified polyol process: Synthesis, characterization, and magnetic properties. *Journal of Colloid and Interface Science*, 311(2), 461–468. doi: 10.1016/j.jcis.2007.03.045

- De Groot, S. R., & Mazur, P. (1984). *Non-equilibrium thermodynamics*. Courier Dover Publications.
- Evans, D.F., Wennerstrom, H. (1999). The Colloidal Domain: Where physics, chemistry, biology and technology meet. In *The Colloidal Domain: Where physics, chemistry, biology and technology meet*.
- Everett, D. H. (1988). *Basic principles of colloid science* (Vol. 144). Royal Society of Chemistry London.
- Favilla, P. C., Acosta, J. J., Schvezov, C. E., Sercovich, D. J., & Collet-Lacoste, J. R. (2013). Size control of carbon-supported platinum nanoparticles made using polyol method for low temperature fuel cells. *Chemical Engineering Science*, 101, 27–34. doi: 10.1016/j.ces.2013.05.067
- Fievet, F., Lagier, J., Blin, B., Beaudoin, B., & Figlarz, M. (1989). Homogeneous and heterogeneous nucleations in the polyol process for the preparation of micron and submicron size metal particles. *Solid State Ionics*, 32–33, 198–205. doi: 10.1016/0167-2738(89)90222-1
- Glansdorff, P., & Prigogine, I. (1971). *Structure, stabilité et fluctuations* (Masson (ed.)). Paris.
- Hei, H., He, H., Wang, R., Liu, X., Zhang, G., Zhao, T., Sun, R., Yu, S., Zhang, Z., Zhou, L., Huang, H., & Du, R. (2010). Size-controlled preparation of silver nanoparticles by a modified polyol method. *Colloids and Surfaces A: Physicochemical and Engineering Aspects*, 366(1–3), 197–202. doi: 10.1016/j.colsurfa.2010.06.005
- Hirai, H., Nakao, Y., & Toshima, N. (1978). Preparation of Colloidal Rhodium in Poly(vinyl Alcohol) by Reduction with Methanol. *Journal of Macromolecular Science: Part A - Chemistry*, 12(8), 1117–1141. doi: 10.1080/00222337808063179
- Hornstein, B. J., & Finke, R. G. (2004). Transition-Metal Nanocluster Kinetic and Mechanistic Studies Emphasizing Nanocluster Agglomeration: Demonstration of a Kinetic Method That Allows Monitoring of All Three Phases of Nanocluster Formation and Aging. *Chemistry of Materials*, 16(1), 139–150. doi: 10.1021/cm034585i
- Hunter, R. J. (1987). Foundations of Colloid Science. In *Foundations of Colloid Science* (Vol. 1).
- Keizer, J. (1982). Nonequilibrium statistical thermodynamics and the effect of diffusion on chemical reaction rates. *The Journal of Physical Chemistry*, 86(26), 5052–5067. doi: 10.1021/j100223a004
- Keizer, J. (1987a). *The Thermodynamics of Nonequilibrium Statistical Processes*. Springer-Verlag, Inc.
- Keizer, J. (1987b). Diffusion effects on rapid bimolecular chemical reactions. *Chemical Reviews*, 87(1), 167–180. doi: 10.1021/cr00077a009
- Khatouri, J., Mostafavi, M., Amblard, J., & Belloni, J. (1993). Ionization potential of clusters in liquids. *Zeitschrift Für Physik D Atoms, Molecules and Clusters für Physik D Atoms, Molecules and Clusters*, 26(1), 82–86. doi: 10.1007/BF01425625
- Kim, B. H., Hackett, M. J., Park, J., & Hyeon, T. (2014). Synthesis, Characterization, and Application of Ultrasmall Nanoparticles. *Chemistry of Materials*, 26(1), 59–71. doi: 10.1021/cm402225z
- Kim, D., Jeong, S., & Moon, J. (2006). Synthesis of silver nanoparticles using the polyol process and the influence of precursor injection. *Nanotechnology*, 17(16), 4019–4024. doi: 10.1088/0957-4484/17/16/004
- Kopple, K., Meyerstein, D., & Meisel, D. (1980). Mechanism of the catalytic hydrogen production by gold sols. Hydrogen/deuterium isotope effect studies. *The Journal of Physical Chemistry*, 84(8), 870–875. doi: 10.1021/j100445a016

- Labib, M. E. (1988). The origin of the surface charge on particles suspended in organic liquids. *Colloids and Surfaces*, 29(3), 293–304. doi: 10.1016/0166-6622(88)80124-0
- LaMer, V. K., & Dinegar, R. H. (1950). Theory, production and mechanism of formation of monodispersed hydrosols. *Journal of the American Chemical Society*, 72(11), 4847–4854.
- Landau, L. D., & Lifshitz, E. M. (1988). *Física estadística* (Vol. 5). Academia de Ciencias URSS. Reverte.
- Liu, H., Song, C., Zhang, L., Zhang, J., Wang, H., & Wilkinson, D. P. (2006). A review of anode catalysis in the direct methanol fuel cell. *Journal of Power Sources*, 155(2), 95–110. doi: 10.1016/j.jpowsour.2006.01.030
- Liu, Z., Hong, L., & Tay, S. (2007). Preparation and characterization of carbon-supported Pt, PtSnO₂ and PtRu nanoparticles for direct methanol fuel cells. *Materials Chemistry and Physics*, 105(2–3), 222–228. doi: 10.1016/j.matchemphys.2007.04.045
- Luo, Y. (2007). One-step preparation of gold nanoparticles with different size distribution. *Materials Letters*, 61(4–5), 1039–1041. doi: 10.1016/j.matlet.2006.06.051
- Mayer, A. B. R., & Mark, J. E. (1997). Transition metal nanoparticles protected by amphiphilic block copolymers as tailored catalyst systems. *Colloid & Polymer Science*, 275(4), 333–340. doi: 10.1007/s003960050090
- Mayer, Andrea B. R., & Mark, J. E. (1997). Comparisons between cationic polyelectrolytes and nonionic polymers for the protection of palladium and platinum nanocatalysts. *Journal of Polymer Science Part A: Polymer Chemistry*, 35(15), 3151–3160. doi: 0.1002/(SICI)1099-0518(19971115)35:15<3151::AID-POLA8>3.0.CO;2-Z
- Mayer, Andrea B.R. (1998). Formation of noble metal nanoparticles within a polymeric matrix: nanoparticle features and overall morphologies. *Materials Science and Engineering: C*, 6(2–3), 155–166. doi: 10.1016/S0928-4931(98)00049-6
- Mayer, Andrea B R, Hausner, S. H., & Mark, J. E. (2000). Colloidal Silver Nanoparticles Generated in the Presence of Protective Cationic Polyelectrolytes. *Polymer Journal*, 32(1), 15–22. doi: 10.1295/polymj.32.15
- Mayer, Andrea B R, Mark, J. E., & Morris, R. E. (1998). Palladium and Platinum Nanocatalysts Protected by Amphiphilic Block Copolymers. *Polymer Journal*, 30(3), 197–205. doi: 10.1295/polymj.30.197
- Molski, A. (1996). Fluctuation theory of the coupling between diffusion and reaction in 1D: coalescence with point reactivities. *Chemical Physics Letters*, 252(1–2), 42–50. doi: http://dx.doi.org/10.1016/S0009-2614(96)00166-2
- Mostafavi, M., Dey, G. R., François, L., & Belloni, J. (2002). Transient and Stable Silver Clusters Induced by Radiolysis in Methanol. *The Journal of Physical Chemistry A*, 106(43), 10184–10194. doi: 10.1021/jp014257a
- Mostafavi, Mehran, Keghouche, N., Delcourt, M.-O., & Belloni, J. (1990). Ultra-slow aggregation process for silver clusters of a few atoms in solution. *Chemical Physics Letters*, 167(3), 193–197. doi: 10.1016/0009-2614(90)85004-V
- Mucalo, M. R., & Cooney, R. P. (1989). F.T.I.R. spectra of carbon monoxide adsorbed on platinum sols. *Journal of the Chemical Society, Chemical Communications*, 2, 94. doi: 10.1039/c39890000094
- Napper, D. H. (1983). *Polymeric stabilization of colloidal dispersions: Vol. 7*. Academic Press London.

Oh, H.-S., Oh, J.-G., & Kim, H. (2008). Modification of polyol process for synthesis of highly platinum loaded platinum–carbon catalysts for fuel cells. *Journal of Power Sources*, 183(2), 600–603. doi: 10.1016/j.jpowsour.2008.05.070

Overbeek, J. T. G., & Goodwin, J. W. (1981). Colloidal dispersions. *Royal Society of Chemistry, London*, 1–23.

Özkar, S., & Finke, R. G. (2002a). Nanocluster formation and stabilization fundamental studies: Ranking commonly employed anionic stabilizers via the development, then application, of five comparative criteria. *Journal of the American Chemical Society*, 124, 5796–5810. doi: 10.1021/ja012749v

Özkar, S., & Finke, R. G. (2002b). Nanocluster Formation and Stabilization Fundamental Studies. 2. Proton Sponge as an Effective H⁺ + Scavenger and Expansion of the Anion Stabilization Ability Series. *Langmuir*, 18(20), 7653–7662. doi: 10.1021/la020225i

Park, B. K., Jeong, S., Kim, D., Moon, J., Lim, S., & Kim, J. S. (2007). Synthesis and size control of monodisperse copper nanoparticles by polyol method. *Journal of Colloid and Interface Science*, 311(2), 417–424. doi: 10.1016/j.jcis.2007.03.039

Peng, S., Lee, Y., Wang, C., Yin, H., Dai, S., & Sun, S. (2008). A facile synthesis of monodisperse Au nanoparticles and their catalysis of CO oxidation. *Nano Research*, 1(3), 229–234. doi: 10.1007/s12274-008-8026-3

Prabhuram, J., Wang, X., Hui, C. L., & Hsing, I.-M. (2003). Synthesis and Characterization of Surfactant-Stabilized Pt/C Nanocatalysts for Fuel Cell Applications. *The Journal of Physical Chemistry B*, 107(40), 11057–11064. doi: 10.1021/jp0357929

Prabhuram, J., Zhao, T. S., Wong, C. W., & Guo, J. W. (2004). Synthesis and physical/electrochemical characterization of Pt/C nanocatalyst for polymer electrolyte fuel cells. *Journal of Power Sources*, 134(1), 1–6. doi: 10.1016/j.jpowsour.2004.02.021

Ross, S., & Morrison, I. D. (1988). Size and surface area. In *Colloidal systems and interfaces*. Wiley, New York.

Roucoux, A., Schulz, J., & Patin, H. (2002). Reduced Transition Metal Colloids: A Novel Family of Reusable Catalysts? *Chemical Reviews*, 102(10), 3757–3778. doi: 10.1021/cr010350j

Rupprechter, G., Kaichev, V. V., Unterhalt, H., Morkel, M., & Bukhtiyarov, V. I. (2004). CO dissociation and CO hydrogenation on smooth and ion-bombarded Pd(111): SFG and XPS spectroscopy at mbar pressures. *Applied Surface Science*, 235(1–2), 26–31. doi: 10.1016/j.apsusc.2004.05.120

Todorova, M., Lundgren, E., Blum, V., Mikkelsen, A., Gray, S., Gustafson, J., Borg, M., Rogal, J., Reuter, K., Andersen, J. N., & Scheffler, M. (2003). The Pd(1)–R27°–O surface oxide revisited. *Surface Science*, 541(1–3), 101–112. doi: 10.1016/S0039-6028(03)00873-2

Torigoe, K., Remita, H., Beaunier, P., & Belloni, J. (2002). Radiation-induced reduction of mixed silver and rhodium ionic aqueous solution. *Radiation Physics and Chemistry*, 64(3), 215–222. doi: 10.1016/S0969-806X(01)00453-4

Turkevich, J., Stevenson, P. C., & Hillier, J. (1951). A study of the nucleation and growth processes in the synthesis of colloidal gold. *Discuss. Faraday Soc.*, 11(0), 55–75. doi: 10.1039/DF9511100055

Turkevich, J., Stevenson, P. C., & Hillier, J. (1953). The formation of colloidal gold. *The Journal of Physical Chemistry*, 57(7), 670–673.

Watzky, M. A., & Finke, R. G. (1997). Transition Metal Nanocluster Formation Kinetic and Mechanistic Studies. A New Mechanism When Hydrogen Is the Reductant: Slow, Continuous Nucleation and Fast Autocatalytic Surface Growth. *Journal of the American Chemical Society*, 119(43), 10382–10400. doi: 10.1021/ja9705102

Watzky, M. A., Finney, E. E., & Finke, R. G. (2008). Transition-metal nanocluster size vs formation time and the catalytically effective nucleus number: a mechanism-based treatment. *Journal of the American Chemical Society*, 130(36), 11959–11969. doi: 10.1021/ja8017412

Widegren, J. a., Aiken, J. D., Özkar, S., & Finke, R. G. (2001). Additional Investigations of a New Kinetic Method To Follow Transition-Metal Nanocluster Formation, Including the Discovery of Heterolytic Hydrogen Activation in Nanocluster Nucleation Reactions. *Chemistry of Materials*, 13(2), 312–324. doi: 10.1021/cm0006852

Wu, S. H., & Chen, D. H. (2003). Synthesis and characterization of nickel nanoparticles by hydrazine reduction in ethylene glycol. *Journal of Colloid and Interface Science*, 259(2), 282–286. doi: 10.1016/S0021-9797(02)00135-2

Yan, J., Zou, G., Wang, X., Bai, H., Mu, F., & Wu, A. (2011). Large-scale synthesis of Ag nanoparticles by polyol process for low temperature bonding application. *ICEPT-HDP 2011 Proceedings - 2011 International Conference on Electronic Packaging Technology and High Density Packaging*, 254–259. doi: 10.1109/ICEPT.2011.6066831

Yano, H., Kataoka, M., Yamashita, H., Uchida, H., & Watanabe, M. (2007). Oxygen reduction activity of carbon-supported Pt-M (M = V, Ni, Cr, Co, and Fe) alloys prepared by nanocapsule method. *Langmuir: The ACS Journal of Surfaces and Colloids*, 23(11), 6438–6445. doi: 10.1021/la070078u

Zhou, W., Zhou, Z., Song, S., Li, W., Sun, G., Tsiakaras, P., & Xin, Q. (2003). Pt based anode catalysts for direct ethanol fuel cells. *Applied Catalysis B: Environmental*, 46(2), 273–285. doi: 10.1016/S0926-3373(03)00218-2

SOBRE EL ORGANIZADOR

El Dr. Juan Ramón Collet-Lacoste es licenciado en ciencias químicas de la Universidad de Buenos Aires (UBA) y PhD de la Universidad de Paris Sud (XI). Su especialidad es la físico química, en la rama de la termodinámica de los procesos irreversibles (TPI), especialmente en el estudio de los procesos cinéticos en los sistemas electroquímicos.

Ha desarrollado varios trabajos relacionados a los mecanismos de reacción y transporte de materia sobre electrodos metálicos, así como el desarrollo de electrodos para celdas de combustible de baja temperatura (fuel cells).

Es un especialista en la técnica de impedancia electroquímica, en la cual ha publicado varios artículos en revistas internacionales.

Desde el punto de vista experimental, ha trabajado en el desarrollo de celdas de combustible con Nps de platino y paladio y de electrolizadores alcalinos de baja temperatura.

Actualmente realiza trabajos sobre la oxidación acuosa del aluminio en gradientes de temperatura. Este trabajo esta relacionado a los elementos combustibles de los reactores experimentales multipropósito para la fabricación de radioisótopos de uso médico.

ÍNDICE REMISSIVO

A

Antiseptics 126, 127

Aquatic environment 98, 99, 100, 101

Au Nanoparticle 87, 96

B

Bactericidal 126, 127

Bioremediation 98, 99, 100, 101, 105, 106, 125

Biosíntesis extracelular 116

Biosíntesis intracelular 116

C

Carbon nanoparticles 99, 101, 104, 135, 136, 137, 138, 139, 142

Catálise 29, 62, 63, 64, 66, 67, 81

Cerâmicas funcionais 28

Contaminants 98, 99, 100, 101, 102

Controlled release 126

E

Efeito Plasmônico 62, 71, 76, 77, 80, 81, 82, 83

Extracto 108, 109, 110, 111, 112, 113, 120

F

Feixe de elétrons 49, 52, 53, 54, 55, 56, 57

Filtradhussao extracelular 116

Filtrado libre de células 116, 118, 120, 121, 122, 123, 124

Fotocatálise 61, 62, 64, 66, 67, 68, 70, 71, 72, 78, 80, 81, 82, 83

H

Hidrotermal assistido por micro-ondas 28, 29

Hongo 108, 109, 111, 113, 116, 117, 118, 119, 120, 121, 122, 123, 124

Hybrid film 87, 88, 89, 90, 91, 92, 93, 95

L

Low temperature fuel cells 1, 24

M

Metais nobres 61, 62, 68, 69, 83

N

Nanofiber 48, 87, 88, 91, 92, 93, 94, 95, 96, 101

Nanomateriais 34, 39, 54, 57

Nanoparticles 1, 2, 23, 24, 25, 26, 27, 29, 38, 39, 40, 48, 58, 59, 62, 84, 85, 87, 88, 93, 94, 95, 98, 99, 100, 101, 102, 103, 104, 105, 106, 107, 109, 114, 115, 116, 124, 125, 126, 127, 128, 129, 130, 131, 132, 133, 134, 135, 136, 137, 138, 139, 140, 142

Nanoparticles synthesis 1, 85

Nanopartículas 28, 34, 37, 39, 40, 41, 42, 43, 46, 47, 54, 61, 64, 67, 68, 70, 72, 76, 83, 85, 108, 109, 110, 111, 112, 113, 114, 116, 117, 118, 119, 121, 122, 123, 124, 125, 134

Nanopartículas Metálicas 39, 40, 54, 61, 62, 68, 83

Nanotechnology 24, 59, 87, 96, 125, 126, 141, 142

Nucleation and growth mechanism 1

O

Óxido de cério 28, 29, 30, 31, 32, 33, 37, 38

Óxido de grafeno reduzido 49, 50, 51, 52, 53, 54, 56

P

Plant probiotics 135

Praseodímio 28, 30, 33, 37

Prata 31, 39, 40, 41, 47, 70, 82, 85

Puntos cuánticos 109, 111

R

Radiação gama 49, 52, 53, 56, 57, 59

Radiação ionizante 49, 52, 53, 54

S

Self-assembly 87, 88, 91, 95, 96

SERS 39, 40, 42, 46, 47, 48

Soil 99, 135, 136, 137, 138, 139, 141

T

Tetramethylbenzidine 87, 96

Thermodynamic properties 1

Transition metals 1, 3, 12, 22

V

Vegetable 135

Virucidal and bioactive compounds 126